



Methanol permeability and performance of Nafion–zirconium phosphate composite membranes in active and passive direct methanol fuel cells

C. Arbizzani^a, A. Donnadio^b, M. Pica^b, M. Sganappa^b, A. Varzi^a, M. Casciola^{b,*}, M. Mastragostino^a

^a University of Bologna, Department of Metal Science, Electrochemistry and Chemical Techniques, Via San Donato 15, 40127 Bologna, Italy

^b University of Perugia, Department of Chemistry, Via Elce di Sotto 8, 06123 Perugia, Italy

ARTICLE INFO

Article history:

Received 5 June 2009

Received in revised form 6 July 2009

Accepted 7 July 2009

Available online 24 July 2009

Keywords:

Methanol permeability

Proton conductivity

Swelling

Active DMFC

Passive DMFC

ABSTRACT

Methanol crossover through polymer electrolyte membranes represents one of the major problems to be solved in order to improve direct methanol fuel cell (DMFC) performance. With this aim, Nafion/zirconium phosphate (ZrP) composite membranes, with ZrP loading in the range 1–6 wt%, were prepared by casting from mixtures of gels of exfoliated ZrP and Nafion 1100 dispersions in dimethylformamide. These membranes were characterised by methanol permeability, swelling and proton conductivity measurements, as well as by tests in active and passive DMFCs in the temperature range 30–80 °C. Increase in filler loading results in a decrease in both methanol permeability and proton conductivity. As a consequence of the reduced conductivity the power density of active DMFCs decreases with increasing ZrP loading (from 46 to 32 mW cm⁻² at 80 °C). However, due to the lower methanol permeability, the room temperature Faraday efficiency of passive DMFCs, with 20 mA cm⁻² discharge current, nearly doubles when Nafion 1100 is replaced by the composite membrane containing 4 wt% ZrP.

© 2009 Elsevier B.V. All rights reserved.

1. Introduction

High aspect ratio particles arising from the exfoliation of layered solids are widely used as fillers of polymers in order to reduce the permeability of gaseous or liquid species in the polymeric matrix [1]. The presence of the filler increases the tortuosity of the diffusion paths of the permeating species: in particular, the larger the exfoliation degree of the filler and its aspect ratio, the greater is the barrier raised by the filler to diffusion. This approach was used to reduce the methanol permeability of Nafion membranes of direct methanol fuel cells (DMFCs) which suffer from the high methanol crossover through the polymer [2,3].

In order to lower methanol permeability while keeping high proton conductivity the filler should be itself a proton conductor and α -layered zirconium phosphate (hereafter ZrP) is an attractive filler. It displays good thermal and chemical stability, high proton conductivity (up to 10⁻² Scm⁻¹ when completely exfoliated and fully hydrated [4]) and the possibility to obtain nanoparticles with high aspect ratio [5,6].

Compared with neat Nafion, Nafion/ZrP composite membranes are characterised by an enhanced elastic modulus [7–9], which is likely responsible for their better dimensional stability at high

temperature and high relative humidity (RH) that allows fuel cell operation above 100 °C [10–12]. Nafion/ZrP membranes for DMFCs are generally prepared by growing nanosized ZrP within the pre-formed ionomeric matrix through ion exchange of the ionomer protons with zirconium cationic species, and subsequent treatment with an aqueous solution of phosphoric acid [10–16]. While these membranes display lower methanol permeability than neat Nafion, they perform worse in DMFCs fed with low methanol concentrations [11,14,15], with the only exception of the Nafion 115/ZrP membrane reported in Ref. [10].

A different synthetic approach is based on the casting of mixtures of a Nafion solution and a dispersion [17] or gel [18] of exfoliated ZrP. A reduction of methanol permeability by a factor of 10 was observed even for ZrP loadings as low as 2 wt% when microcrystalline ZrP synthesized by direct precipitation from HF solutions was used as starting material for the gels of exfoliated ZrP [18].

The present paper deals with Nafion/ZrP membranes prepared according to the latter synthetic route, where the starting ZrP microcrystals were grown by refluxing amorphous ZrP in phosphoric acid: as a consequence the average crystal size (0.2–0.4 μ m) was considerably smaller than that of ZrP precipitated from HF solutions (5–10 μ m) [18,19]. Membranes with ZrP loadings of 2, 4 and 6 wt% (hereafter Nafion/ZrP_x, with $x=2, 4, 6$) were characterised in terms of methanol permeability, proton conductivity and swelling behaviour, and tested in active and passive DMFCs.

* Corresponding author. Tel.: +39 075 5855567; fax: +39 075 5855566.
E-mail address: macs@unipg.it (M. Casciola).

2. Experimental

2.1. Chemicals

Zirconyl propionate ($\text{ZrO}_{1.27}(\text{C}_2\text{H}_5\text{COO})_{1.46}$, MW = 218 Da) was supplied by Magnesium Elektron Ltd., England and ortho phosphoric acid (99%) by Fluka. The Nafion dispersion (EW = 1100, 20 wt% in a mixture of aliphatic alcohols and water) and all the other reagents were supplied by Aldrich. The concentration of the Nafion dispersion was accurately determined by potentiometric titration with 0.1 M NaOH.

2.2. Preparation of ZrP

An aqueous solution of 0.5 M $\text{ZrOCl}_2 \cdot 8\text{H}_2\text{O}$ and 4 M HCl was added drop by drop to a solution of 2 M H_3PO_4 so that the P/Zr molar ratio was 11. The precipitate thus obtained was left at rest for 2 days, washed four times with 0.4 M H_3PO_4 (about 10 mL washing solution per gram of solid), three times with water and refluxed in 7 M H_3PO_4 for 60 h. The solid was then washed several times with 0.01 M HCl (until the H_3PO_4 concentration in the washing solution was lower than 3×10^{-4} M), and finally with deionised water. The solid was dried in air and stored at 53% relative humidity. The physicochemical characterisation of this material (including SEM pictures) was already reported in Ref. [19].

2.3. Preparation of ZrP gels

A colloidal dispersion of ZrP intercalated with propylamine in water was prepared according to Ref. [5] by adding 16.6 mL of 0.1 M propylamine to a suspension of 0.5 g ZrP in 33 mL water under ultrasound treatment (100 mL for 40 min, at 22 kHz, ~30 W). The dispersion was left under stirring at room temperature for 24 h and then treated with 6 mL of 1 M HCl (pH < 2) so as to regenerate the hydrogen form of zirconium phosphate. The solid was separated from the solution and washed with water under vigorous stirring. A gelatinous precipitate settled by centrifugation at 3000 rpm. Washing was repeated up to the elimination of chloride ions. An amount of the ZrP gel in water, containing 1.5–2.5 wt% anhydrous ZrP and x mL water, was washed three times with 4x mL of dimethylformamide (DMF). After each washing, the ZrP gel was separated from the solution by centrifuging at 3000 rpm. The final gelatinous product contained 3–4 wt% anhydrous ZrP in DMF.

2.4. Preparation of Nafion/ZrP composite membranes

5 g of the commercial Nafion dispersion were concentrated at 80 °C so as to reduce the volume by 90%. About 10 mL of DMF was added to the remaining solution and the volume was reduced again. The procedure was repeated several times in order to assure the complete removal of water and alcohols. The final dispersion contained about 15 wt% Nafion in DMF. A weighed amount of ZrP gel in DMF was added to the polymer solution and the mixture was held under stirring at room temperature for about 5 h and cast on a Petri dish. The solvent was evaporated at 100 °C overnight. Finally, the composite membranes were washed with a 1 M HCl solution at room temperature for 24 h and then heated at 100 °C for 4 h. Composite membranes with filler contents in the range 2–6 wt% and thickness between 190 and 200 nm were prepared. Neat recast Nafion membranes, to be used as reference, were also prepared under the same synthetic procedure.

2.5. Active and passive DMFCs

Membrane electrode assemblies (MEAs) were prepared using home-made anodes, obtained by spraying iso-propanol based inks

containing a carbon/PtRu catalyst onto a Carbon Cloth GDL (ELAT®-GDL). The PtRu supported on home-made mesoporous carbon with pore size distribution centred in the range 35–65 nm provides a good catalytic activity for methanol oxidation as reported in Ref. [20]. The Pt content of the anodes ranged from 1.0 to 1.25 mg cm^{-2} . The cathodes were commercial ELAT® V 2.1 Gas Diffusion Electrode (GDE) with Pt black loading of 5.0 mg cm^{-2} . The electrodes were hot-pressed (1000 psi at 125 °C for 120 s) with the composite membranes to give the MEAs.

MEAs were assembled in passive DMFCs, which were held together by two acrylic plates with fixed stainless-steel current collectors. The electrode area was 3 cm^2 . A reservoir (1.4–1.7 mL) filled with 1 M CH_3OH solution fuelled the anode while the air diffused into the cathode through the openings of the cathode plate. Before testing the passive DMFCs underwent activation by 1000 galvanostatic steps, at room temperature (RT), between open circuit condition (120 s) and high constant current (60 s), refreshing the CH_3OH solution in the reservoir every 100–150 steps.

MEAs for active DMFCs were installed in an electrochem fuel cell test-fixtured connected to an Electrochem MTS-A-150/EC-DM test-station. The electrode area was 5 cm^2 . A 1 M CH_3OH solution, at the same temperature as the cell and at atmospheric pressure, fed the anode compartment and dry O_2 at 1 bar and RT fed the cathode. CH_3OH and O_2 flow rates were 5 and 250 mL min^{-1} and the tests were performed at 30, 60 and 80 °C. Before testing, the active DMFCs underwent activation at high current at 80 °C for 4 h and, after temperature changes, the conditioning time under reactant fluxes was 30 min.

Chronoamperometry tests (CA) at different cell potentials (300 s at each potential followed by 300 s in OCV) were performed to build the polarisation curves for both active and passive DMFCs. Chronopotentiometry tests (CP) at different currents and open circuit voltage (OCV) measurements were also performed for several hours to highlight the methanol crossover in the passive DMFCs. The CH_3OH solution in passive DMFCs was renewed before starting every CA set of measurements at different potentials, CP test and OCV measurement over time.

All the DMFC electrochemical tests were performed with multichannel Bio-Logic VSP and VMP potentiostat/galvanostats, the latter equipped with 2 and 10 A boosters.

2.6. Methanol permeability measurements

In active DMFCs methanol permeability was determined on the basis of the steady state limiting current density (i_{lim}) resulting from complete electro-oxidation of permeating methanol at the cathode side, as described in Ref. [21]. Methanol permeability, defined as the product between methanol diffusion coefficient (D_m) and methanol concentration at the feed edge (C_m), was calculated by the equation:

$$D_m C_m = \frac{i_{\text{lim}} L}{6F}$$

where L is the membrane thickness. Steady state limiting current density (i_{lim}) was measured both by CA at 0.7 V after 300 s, and by linear sweep voltammetry (LSV) up to 1 V with 1 mV s^{-1} scan rate; in this case i_{lim} was reached at 0.8 V.

2.7. Swelling tests

Membrane discs, 25 mm in diameter and ~0.2 mm in thickness, were dried overnight at 80 °C under a dry nitrogen flow and then immersed for 15 h in a 1 M methanol solution at constant temperature. The membrane swelling, both in the in-plane (S_{ip}) and in the

Table 1

Permeability ($D_m C_m$) for Nafion 1100 and Nafion/ZrP composite membranes as a function of temperature. $D_m C_m$ values were calculated from the steady state limiting current values obtained from chronoamperometry (CA) and linear sweep voltammetry (LSV).

Membrane	Thickness (μm)	T ($^{\circ}\text{C}$)	$D_m C_m$ (LSV) ($\text{mol cm}^{-1} \text{s}^{-1} \times 10^{10}$)	$D_m C_m$ (CA) ($\text{mol cm}^{-1} \text{s}^{-1} \times 10^{10}$)
Nafion 1100	200	30	16	13
		60	35	30
		80	54	42
Nafion/ZrP2	195	30	12	10
		60	27	24
		80	38	31
Nafion/ZrP4	210	30	10	9
		60	21	19
		80	28	23
Nafion/ZrP6	200	30	9	8
		60	21	18
		80	–	–

through-plane directions (S_{tp}) was calculated by the relation:

$$S_{ip} \text{ or } S_{tp} = 100 \times (x/x_0) - 1$$

where x_0 and x are the membrane dimensions, in the in-plane or in the through-plane direction, of the dry and swollen membrane, respectively. Similarly, volume swelling (S_v) was calculated by the relation:

$$S_v = 100 \times (V/V_0) - 1$$

where V_0 and V are the volumes of the dry and swollen membrane.

2.8. Conductivity measurements

The through-plane conductivity of the membranes was determined by impedance measurements as described in Ref. [22]. The membrane was sandwiched between gas diffusion electrodes (ELAT containing 1 mg cm^{-2} Pt loading) with a pressure of 60 kg cm^{-2} , which was not further controlled during the experiment.

3. Results and discussion

3.1. Methanol permeability

The methanol permeability of Nafion 1100 and Nafion/ZrP membranes (Table 1) was calculated from the limiting current values obtained from CA and LSV. The data from LSV are higher than those from CA by about 10–25%, presumably because in CA the limiting current was not completely reached at 0.7 V. However, the relative permeability (P_r , defined as the ratio of the composite membrane permeability to the Nafion 1100 permeability) is about the same from CA and LSV data, as shown in Fig. 1 where average P_r values are plotted as a function of temperature, and the error bar represents the difference between P_r from CA and LSV. The P_r value decreases with increasing the filler loading from 2 to 6 wt% and is nearly independent of temperature for Nafion/ZrP2 and Nafion/ZrP6. By contrast, a non-negligible decrease in P_r (from 0.66 to 0.53) was observed for Nafion/ZrP4 with increasing temperature.

The lowest P_r value ($P_r = 0.53$) found at 80°C for Nafion/ZrP4 is comparable with the value (~ 0.5) reported in the literature for Nafion 115 and Nafion 117 membranes filled with 23–26 wt% in situ grown ZrP [11,15]. Therefore the same permeability decrease is achieved with a much lower amount of filler when exfoliated ZrP is used instead of in situ grown ZrP. On the other hand, the P_r values here reported for membranes with 2 and 4 wt% filler loadings are significantly higher than those found for similar Nafion/ZrP membranes ($P_r = 0.10$ – 0.18) prepared by exfoliation of larger ZrP crystals (average size 5– $10 \mu\text{m}$ [18]) than those used in the present work (average size 0.2– $0.4 \mu\text{m}$). This is likely due to the fact that the

larger the layered crystals, the higher is the aspect ratio of the particles resulting from their exfoliation and the more tortuous is the methanol diffusion paths through the composite membrane. Thus, filler morphology seems to be a key factor for methanol permeability.

3.2. Swelling

The through-plane (S_{tp}), in-plane (S_{ip}) and volume swelling (S_v) values in 1 M methanol solutions were determined for neat Nafion 1100 and for the composite membranes containing 2 and 6 wt% ZrP in the temperature range 30 – 80°C (Table 2). All these values increase with temperature and, at the same temperature, the membrane swelling is anisotropic, S_{tp} being generally higher than S_{ip} . Moreover, comparison between neat Nafion and the composite membranes shows that the presence of the filler increases the through-plane swelling and decreases the in-plane one, thus enhancing the swelling anisotropy. S_{tp}/S_{ip} ratios lie in the ranges 1.6–2.3 for neat Nafion 1100, 2.6–3.0 for Nafion/ZrP2 and 2.9–3.9 for Nafion/ZrP6. The different influence of the filler on S_{tp} and S_{ip} suggests that the lamellar ZrP particles are mostly oriented with their flat surface parallel to the membrane surface. Due to the opposite changes caused by the filler in S_{tp} and S_{ip} , S_v does not change appreciably for nearly all the investigated samples. This behaviour is different from that observed for Nafion 115 membranes filled with 23 wt% in situ grown ZrP [15], where the filler reduces the uptake of 1 M methanol solution from 36 to 29 wt%.

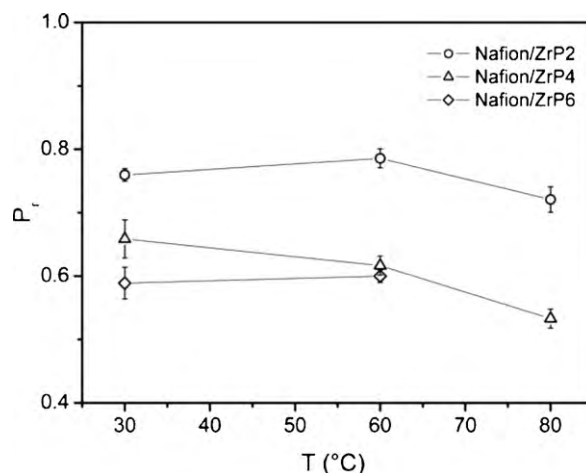


Fig. 1. Relative permeability for Nafion/ZrP composite membranes as a function of temperature.

Table 2
In-plane (S_{ip}), through-plane (S_{tp}) and volume (S_v) swelling in 1 M methanol solutions for the indicated membranes as a function of temperature.

T (°C)	Nafion 1100			Nafion/ZrP2			Nafion/ZrP6		
	S_{ip} (%)	S_{tp} (%)	S_v (%)	S_{ip} (%)	S_{tp} (%)	S_v (%)	S_{ip} (%)	S_{tp} (%)	S_v (%)
30	12.0	20	50.5	8.6	26.3	49.0	9.0	26.3	50.0
40	13.4	21.1	55.6	10.0	26.3	52.9	9.3	–	–
60	14.5	26.3	65.6	10.4	31.6	60.4	9.3	33.3	59.4
80	16.0	36.8	84.1	15.6	44.7	93.5	12.3	47.6	86.2

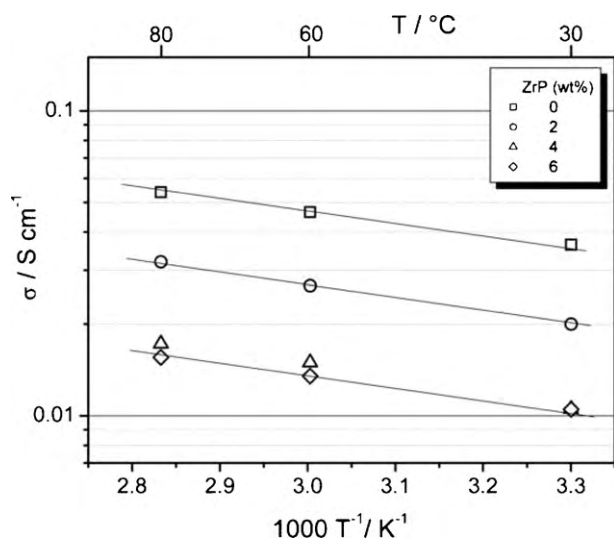


Fig. 2. Proton conductivity as a function of temperature for Nafion 1100 and Nafion/ZrP membranes.

3.3. Proton conductivity

Through-plane conductivity measurements were carried out on neat Nafion 1100 and on Nafion/ZrP composite membranes immersed in 1 M methanol solution so as to reproduce as much as possible the membrane solvation in the fuel cell. In Fig. 2 conductivity data, collected in the range 30–80 °C, are plotted as a function of reciprocal absolute temperature. The slope of the $\log(\sigma)$ versus $1000/T$ straight lines is independent of filler loading, within experimental errors, thus indicating that the activation energy of proton transport ($7.8 \pm 0.7 \text{ kJ mol}^{-1}$) is not affected by the presence of the filler. However, at constant temperature, the conductivity decreases with increasing ZrP loading. Nafion/ZrP6 is by about four times less conductive than Nafion 1100: specifically, at 30 °C, $\sigma = 0.036 \text{ S cm}^{-1}$ for Nafion 1100 and $\sigma = 0.010 \text{ S cm}^{-1}$ for Nafion/ZrP6. Thus the filler just makes the conduction paths more tortuous without affecting the proton transport mechanism. From Figs. 1 and 2 it can be observed that the composite membranes containing 4 and 6 wt% ZrP are characterised by similar values of methanol permeability and proton conductivity.

The present results cannot be directly compared with literature data because none of the previous papers reported ex situ conductivity measurements for Nafion membranes immersed in

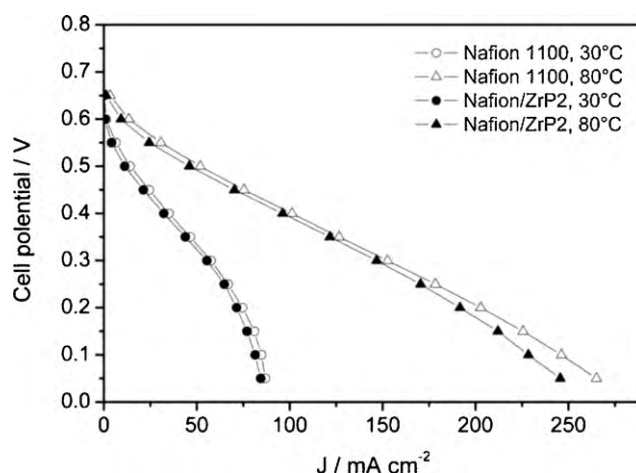


Fig. 3. Polarisation curves at 30 and 80 °C for active DMFCs based on Nafion 1100 and Nafion/ZrP2 membranes.

methanol solutions. However, the values of activation energy and the fact that they are not affected significantly by the filler compare favourably with what reported for Nafion 115 membranes filled with 23 wt% in situ grown ZrP [23]. Moreover the proportional decrease in conductivity determined by the presence of the filler ($\sim 75\%$ for Nafion/ZrP6) is higher than that found, at RH close to 100%, for Nafion membranes containing 20–23 wt% in situ grown ZrP [11,15,23]. Therefore, in spite of the lower filler loading, the tortuosity of the conduction pathways in the composite membrane is greater when the filler is obtained by exfoliation of ZrP microcrystals.

3.4. Active DMFCs

The polarisation curves of active DMFCs based on Nafion 1100 and on composite Nafion/ZrP membranes were collected at 30, 60 and 80 °C. Fig. 3 compares the polarisation curves of the best composite membrane (Nafion/ZrP2) with those of Nafion 1100, at 30 and 80 °C. Table 3 displays the maximum values of power density that decrease with the increase in filler loading. On the basis of the data of methanol permeability and membrane conductivity it can be concluded that changes in the latter are mainly responsible for the observed dependence of fuel cell performance on filler loading.

Similar trends were reported for DMFCs based on Nafion 117/ZrP membranes, working at 130 °C with 1 M methanol [11] and

Table 3
Maximum power density (P_{max}) and corresponding current density (J) values, as a function of temperature, for active DMFCs based on Nafion 1100 and on Nafion/ZrP composite membranes.

Filler loading (wt%)	$T = 30^\circ\text{C}$		$T = 60^\circ\text{C}$		$T = 80^\circ\text{C}$	
	J (mA cm ⁻²)	P_{max} (mW cm ⁻²)	J (mA cm ⁻²)	P_{max} (mW cm ⁻²)	J (mA cm ⁻²)	P_{max} (mW cm ⁻²)
0	58	17.3	120	35.9	153	45.8
2	56	16.6	110	32.8	148	43.9
4	48	14.3	94	27.5	134	33.4
6	46	13.8	94	27.5	127	32.1

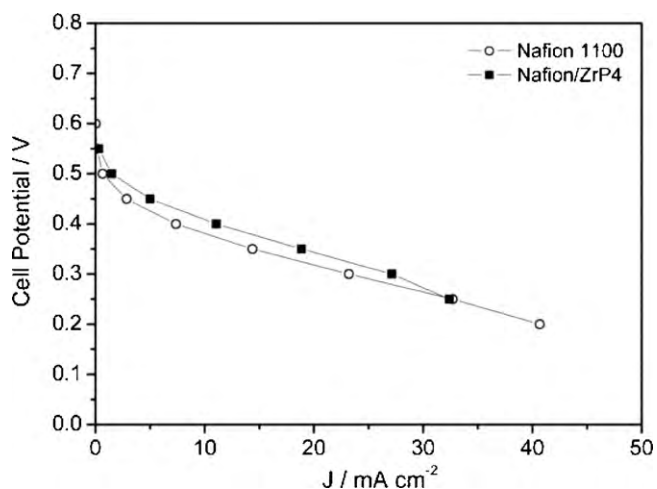


Fig. 4. Polarisation curves for passive DMFCs based on Nafion 1100 and Nafion/ZrP4 membranes at room temperature.

on porous polytetrafluoroethylene impregnated with Nafion/ZrP, working up to 90 °C with 2 M methanol [16]. On the other hand, DMFCs based on Nafion 115/ZrP23 working at 75 °C show slightly better performance than neat Nafion 115 ($\sim 95 \text{ mW cm}^{-2}$ versus $\sim 90 \text{ mW cm}^{-2}$) when fed with 5 M methanol and much better performance ($\sim 75 \text{ mW cm}^{-2}$ versus $\sim 42 \text{ mW cm}^{-2}$) when fed with 10 M methanol [15]. All these results seem to indicate that DMFC performance benefits significantly from reduced methanol crossover only for methanol concentration higher than 5 M.

Finally, it can be observed that the MEA resistance per square centimetre, estimated from the slope of the linear region of the polarisation curve ($\sim 4.3\text{--}5.7 \Omega \text{ cm}^2$ at 30 °C and $\sim 2.0\text{--}2.5 \Omega \text{ cm}^2$ at 80 °C), is higher than the corresponding membrane resistance calculated on the basis of the data of Fig. 2 ($\sim 0.6\text{--}2.1 \Omega \text{ cm}^2$ at 30 °C and $\sim 0.4\text{--}1.4 \Omega \text{ cm}^2$ at 80 °C) thus indicating that the polarisation curves are dominated to a large extent by the resistance of the electrode–electrolyte interface.

3.5. Passive DMFCs

The polarisation curves of passive DMFCs based on neat Nafion 1100 and on Nafion/ZrP membranes are very similar: Fig. 4 compares Nafion 1100 with the best composite membrane (Nafion/ZrP4). As expected, these cells are less performant than active DMFCs with maximum power density values in the range from 6 to 8 mW cm^{-2} .

OCV values are plotted in Fig. 5 as a function of time. Self-discharge times, calculated by extrapolating the decay region of OCV to the time axis, range from 32 h (Nafion 1100) to 55 h (Nafion/ZrP6) and increase with the ZrP loading. These changes in the self-discharge time are consistent with the permeability data measured at 30 °C. In fact, if fuel volume, membrane thickness and active MEA surface are the same, then the ratio of discharge times ($55/32 = 1.7$) is expected to be equal to the reciprocal of the corresponding permeability ratio (1.70 ± 0.08).

The discharge behaviour of the passive DMFCs at constant current density of 10 and 20 mA cm^{-2} is shown in Figs. 6 and 7. Also in this case the discharge time of the DMFCs based on the composite membranes is significantly longer than that of neat Nafion 1100. A more quantitative comparison between the fuel cell performances can be made by calculating the Faraday efficiency of the fuel cell (η_F). On the basis of the data of Figs. 6 and 7 and of the corresponding volumes of the feed methanol solutions ($1.60 \pm 0.05 \text{ mL}$), η_F was roughly evaluated as the ratio of the charge passed at constant current until fuel exhaustion to the charge arising from complete fuel

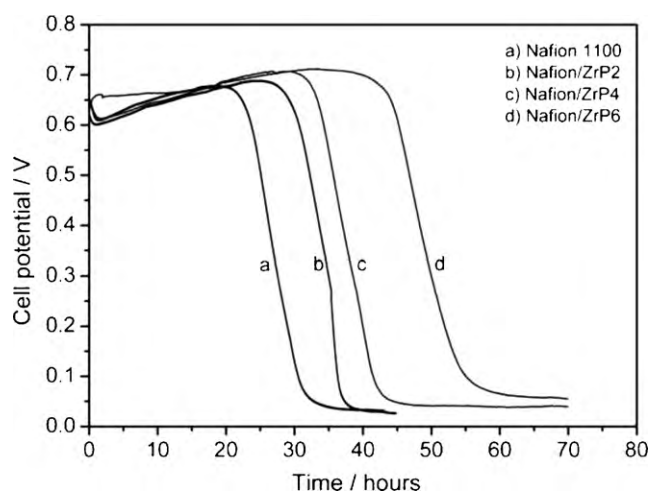


Fig. 5. OCV as a function of time at room temperature for passive DMFCs based on Nafion 1100 and Nafion/ZrP membranes.

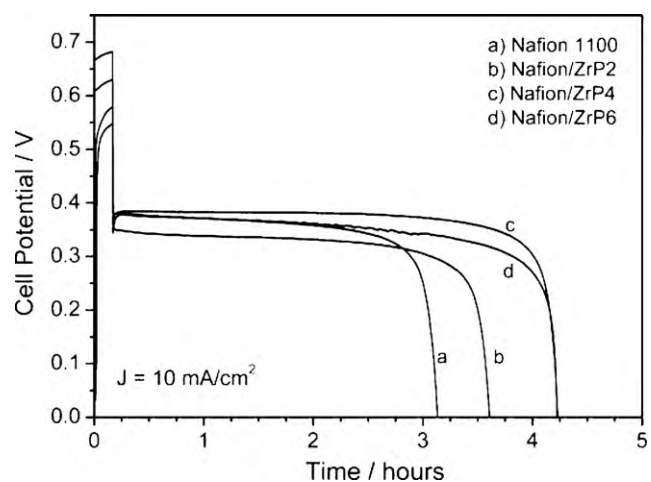


Fig. 6. Discharge behaviour at 10 mA cm^{-2} of passive DMFCs based on Nafion 1100 and Nafion/ZrP membranes.

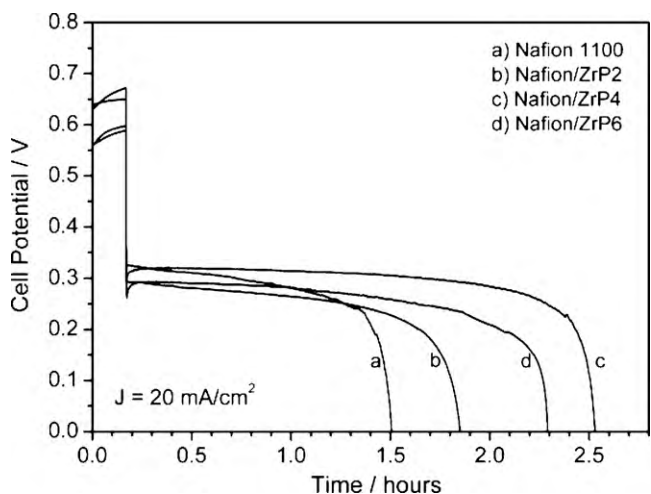


Fig. 7. Discharge behaviour at 20 mA cm^{-2} of passive DMFCs based on Nafion 1100 and Nafion/ZrP membranes.

Table 4
Faraday efficiency (η_F), at 10 and 20 mA cm⁻², of passive DMFCs based on Nafion 1100 and on Nafion/ZrP composite membranes.

Filler loading (wt%)	η_F (%) at 10 mA cm ⁻²	η_F (%) at 20 mA cm ⁻²
0	33	31
2	40	38
4	51	59
6	47	53

oxidation [24]. The data listed in Table 4 show that η_F increases with filler loading in the range 0–4%, the maximum η_F value (59%) being about double of the corresponding value (31%) found for Nafion 1100.

4. Conclusion

Composite Nafion/ZrP membranes, prepared by using gels of exfoliated zirconium phosphate, exhibit reduced methanol permeability that, at best, is about half that of neat Nafion 1100. These results are similar to those already reported in the literature for much higher contents of in situ grown zirconium phosphate and show the importance of the type of synthetic approach and filler morphology against methanol permeability. It is also shown that the swelling of the composite membranes is more anisotropic than that of neat Nafion 1100.

The decrease in proton conductivity of the Nafion/ZrP membrane gives rise to power density of active DMFCs based on these membranes lower than that of DMFCs based on neat Nafion. On the other hand, the reduced methanol permeability of the composite membranes nearly doubles the Faraday efficiency of passive DMFCs when Nafion 1100 is replaced by the composite membrane containing 4 wt% ZrP.

Acknowledgement

This work was supported by MIUR within the FISR 2001 project “Sviluppo di membrane protoniche composite e di configurazioni

elettrodiche innovative per celle a combustibile con elettrolita polimerico” and the PRIN 2007 project “Membrane ibride a conduzione protonica contenenti fosfonati di zirconio lamellari di diversa morfologia e composizione per impieghi in celle a combustibile a elettrolita polimerico”

References

- [1] P.C. LeBaron, Z. Wang, T.J. Pinnavaia, *Appl. Clay Sci.* 15 (1999) 11–29.
- [2] N.W. Deluca, Y.A. Elabd, J. Polym. Sci. Polym. Phys. 44 (2006) 2201–2225.
- [3] V. Neburchilov, J. Martin, H. Wang, J. Zhang, *J. Power Sources* 169 (2007) 221–238.
- [4] M. Casciola, U. Costantino, S. D’Amico, *Solid State Ionics* 22 (1986) 127–133.
- [5] M. Casciola, G. Alberti, A. Donnadio, M. Pica, F. Marmottini, A. Bottino, P. Piaggio, *J. Mater. Chem.* 15 (2005) 4262–4267.
- [6] L. Sun, W.J. Boo, D. Sun, A. Clearfield, H.-J. Sue, *Chem. Mater.* 19 (2007) 1749–1754.
- [7] F. Bauer, M. Willert-Porada, *Solid State Ionics* 177 (2006) 2391–2396.
- [8] G. Alberti, M. Casciola, D. Capitani, A. Donnadio, R. Narducci, M. Pica, M. Sganappa, *Electrochim. Acta* 52 (2007) 8125–8132.
- [9] M. Casciola, D. Capitani, A. Comite, A. Donnadio, V. Frittella, M. Pica, M. Sganappa, A. Varzi, *Fuel Cells* 8 (2008) 217–224.
- [10] C. Yang, S. Srinivasan, A.S. Arico, P. Creti, V. Baglio, *Electrochem Solid-State Lett.* 4 (2001) A31–A34.
- [11] F. Bauer, M. Willert-Porada, *J. Power Sources* 145 (2005) 101–107.
- [12] M.K. Song, Y.T. Kim, J.S. Hwang, H.Y. Ha, H.W. Rhee, *Electrochem. Solid-State Lett.* 7 (2004) A127–A130.
- [13] F. Bauer, M. Willert-Porada, *J. Membr. Sci.* 233 (2004) 141–149.
- [14] F. Bauer, M. Willert-Porada, *Fuel Cells* 6 (2006) 261–269.
- [15] H. Hou, G. Sun, Z. Wu, W. Jin, Q. Xin, *Int. J. Hydrogen Energ.* 33 (2008) 3402–3409.
- [16] L.C. Chen, T.L. Yu, H.L. Lin, S.H. Yeh, *J. Membr. Sci.* 307 (2008) 10–20.
- [17] H.-C. Kuan, C.-S. Wu, C.-Y. Chen, Z.-Z. Yu, A. Dasari, Y.-W. Mai, *Electrochem. Solid-State Lett.* 9 (2006) A76–A79.
- [18] M. Casciola, G. Bagnasco, A. Donnadio, L. Micoli, M. Pica, M. Sganappa, M. Turco, *Fuel Cells*, in press, doi:10.1002/fuce.200800135.
- [19] M. Casciola, A. Donnadio, F. Montanari, P. Piaggio, V. Valentini, *J. Solid State Chem.* 180 (2007) 1198–1208.
- [20] C. Arbizzani, S. Beninati, F. Soavi, A. Varzi, M. Mastragostino, *J. Power Sources* 185 (2008) 615–620.
- [21] X. Ren, T.E. Springer, T.A. Zawodzinski, S. Gottesfeld, *J. Electrochem. Soc.* 147 (2000) 466–474.
- [22] M. Casciola, G. Alberti, M. Sganappa, R. Narducci, *J. Power Sources* 162 (2006) 141–145.
- [23] P. Costamagna, C. Yang, A.B. Bocarsly, S. Srinivasan, *Electrochim. Acta* 47 (2002) 1023–1033.
- [24] D. Chu, R. Jiang, *Electrochim. Acta* 51 (2006) 5829–5835.